

Differential Effects of Serotonin and Dopamine on Human 5-HT_{3A} Receptor Kinetics: Interpretation within an Allosteric Kinetic Model

Ken Solt,¹ Dirk Ruesch,^{1,2} Stuart A. Forman,¹ Paul A. Davies,¹ and Douglas E. Raines¹

¹Department of Anesthesia and Critical Care, Massachusetts General Hospital, Boston, Massachusetts 02114, and ²Department of Anesthesia and Critical Care, University Hospital Giessen-Marburg, Marburg Campus, 35033 Marburg, Germany

Serotonin type 3 (5-HT₃) receptors are members of the pentameric Cys-loop superfamily of receptors that modulate synaptic neurotransmission. In response to agonist binding and unbinding, members of this superfamily undergo a series of conformational transitions that define their functional properties. In this study, we report the results of electrophysiological studies using rapid solution exchange designed to characterize and compare the actions of the high-efficacy agonist serotonin and the low-efficacy agonist dopamine on human 5-HT_{3A} receptors expressed in human embryonic kidney HEK293 cells. In the case of serotonin, receptor activation rates varied with agonist concentration, and deactivation occurred as a single-exponential process with a rate that was similar to the maximal rate of desensitization. Receptors recovered slowly from long desensitizing pulses of serotonin with a sigmoidal time course. In the case of dopamine, receptor activation rates were independent of agonist concentration, receptor deactivation occurred as a complex process that was significantly faster than the maximal rate of desensitization, and recovery from desensitization occurred more quickly than with 5-HT and its time course was not sigmoidal. We developed an allosteric kinetic model for 5-HT_{3A} receptor activation, deactivation, desensitization, and resensitization. Interpretation of our results within the context of this model indicated that the distinct modulatory actions of serotonin versus dopamine are largely attributable to the vastly different rates with which these two agonists induce channel opening and dissociate from open and desensitized states.

Key words: serotonin; dopamine; receptor; kinetic; gating; channel

Introduction

Serotonin type 3 (5-HT₃) receptors are members of the pentameric Cys-loop superfamily of ligand-gated ion channels that also includes the nicotinic acetylcholine, GABA_A, and glycine receptors (Ortells and Lunt, 1995; Reeves and Lummis, 2002). 5-HT₃ receptors are widely distributed throughout the CNS and peripheral nervous system, with particularly high concentrations in the nucleus tractus solitarius, area postrema, and dorsal motor nucleus of the vagus nerve in which they play an important role in mediating emesis (Barnes et al., 1990a,b; Steward et al., 1993). 5-HT₃ receptors are also thought to be important targets of alcohols and to play a role in alcohol addiction (Hodge et al., 2004; Johnson, 2004; McBride et al., 2004). Additionally, 5-HT₃ receptors modulate certain behavioral functions, including cognition, anxiety, and depression, as well as the baroreflex, carotid che-

moreflex, and the Bezold–Jarisch reflex (Costall and Naylor, 2004; Farber et al., 2004; Haus et al., 2004).

Previous electrophysiological and kinetic modeling studies indicate that current activation occurs when 5-HT₃ receptors bind agonist and isomerize from closed to open states (Mott et al., 2001; Hapfelmeier et al., 2003). Activation can apparently occur efficaciously because high concentrations of 5-HT are thought to open nearly all 5-HT₃ receptors. On removal of agonist, currents decay in a process termed deactivation. Currents also decay during continuous agonist exposure, reflecting receptor isomerization to one or more ion-impermeable desensitized states that cannot be activated even by high concentrations of agonist (Reeves et al., 2005; Hu et al., 2006). Such desensitization is reversible because 5-HT₃ receptors resensitize after the removal of agonist. In addition to 5-HT, the neurotransmitter dopamine (DA) can activate 5-HT₃ receptors. Studies using oocyte electrophysiological techniques indicate that, in contrast to 5-HT, DA gates 5-HT₃ receptors with low efficacy because peak currents evoked by receptor-saturating concentrations of DA are significantly smaller than those evoked by 5-HT (Lovinger et al., 2000; Solt et al., 2005). These studies also show that the potency of DA is one to two orders of magnitude lower than that of 5-HT. Because oocyte electrophysiology has relatively low temporal resolution, it cannot resolve other critical aspects of receptor function such as the rates with which agonists induce transitions between

Received Aug. 18, 2007; revised Oct. 10, 2007; accepted Oct. 15, 2007.

This work was supported by National Institutes of Health Grant GM58448 and by a grant from the Foundation for Anesthesia Education and Research. We are grateful to Drs. Jonathan B. Cohen (Harvard Medical School, Boston, MA) and Keith W. Miller (Massachusetts General Hospital, Boston, MA) for their helpful comments during the preparation of this manuscript and to Aiping Liu (Massachusetts General Hospital) for sharing HEK293 cells expressing GABA_A receptors.

Correspondence should be addressed to Dr. Douglas E. Raines, Department of Anesthesia and Critical Care, Massachusetts General Hospital, 55 Fruit Street, Boston, MA 02114. E-mail: draines@partners.org.

DOI:10.1523/JNEUROSCI.3772-07.2007

Copyright © 2007 Society for Neuroscience 0270-6474/07/2713151-10\$15.00/0

different functional states. Single-channel approaches have been helpful in this regard with other ligand-gated ion channels; however, low ion conductivity precludes the use of this technique to study 5-HT_{3A} receptors in detail (Mochizuki et al., 1999; Peters et al., 2005).

In this paper, we report the results of electrophysiological studies using rapid solution exchange designed to characterize and compare the actions of the high-efficacy agonist 5-HT and the low-efficacy agonist DA on human 5-HT_{3A} receptors. Our studies showed that the kinetics with which 5-HT and DA induce receptor activation, deactivation, desensitization, and resensitization are distinct, and we interpreted these results within the context of an allosteric kinetic model of 5-HT_{3A} receptor function.

Materials and Methods

Tissue culture. Human embryonic kidney HEK293 cells were grown in DMEM supplemented with 10% fetal calf serum, 50 U/ml penicillin, and 50 μg/ml streptomycin in a humidified incubator containing 5% CO₂ at 37°C. Cells were grown to 80–90% confluency, harvested using 0.25% trypsin, and gently triturated using a sterile glass pipette. For electrophysiological recordings, cells were grown on 12 mm glass coverslips in 35 mm culture dishes and transiently transfected using the CalPhos Mammalian Transfection kit (Clontech, Mountain View, CA). One microgram of cDNA encoding the human 5-HT_{3A} subunit in the pCDM8 vector (kindly provided by Dr. Ewen Kirkness, J. Craig Venter Institute, Rockville, MD) and 1 μg of green fluorescent protein (GFP) cDNA were used per dish. Cells expressing GFP were identified by fluorescence microscopy and used for electrophysiological recordings 2–5 d after transfection.

Electrophysiological recordings. Before electrophysiological experiments, culture medium was replaced with extracellular solution containing the following (in mM): 140 NaCl, 4.7 KCl, 1.2 MgCl₂, 2.5 CaCl₂, 11 dextrose, and 10 HEPES, adjusted to pH 7.4 with NaOH. All experiments were performed at room temperature (20–22°C). Patch pipettes were pulled from thin-wall filamented 1.5-mm-diameter borosilicate glass (World Precision Instruments, Sarasota, FL), using a P-97 Flaming/Brown Micropipette Puller (Sutter Instruments, Novato, CA). Pipettes were fire polished to open-tip resistances of 2–3 MΩ and filled with intracellular solution containing the following (in mM): 140 KCl, 2 MgCl₂, 10 HEPES, and 11 EGTA, adjusted to pH 7.4 with KOH. All chemicals were purchased from Sigma-Aldrich (St. Louis, MO).

Glass coverslips containing cells were placed in a BT-1-18 recording chamber (Cell MicroControls, Norfolk, VA) and continuously perfused with extracellular solution at a rate of 120 ml/h using an FR-55S flow control valve (Warner Instruments, Hamden, CT). All recordings were performed in the whole-cell configuration unless otherwise indicated, using an Axopatch 200B amplifier (Molecular Devices, Sunnyvale, CA). The smallest round cells expressing GFP were identified and voltage clamped at –60 mV. Compensation was made for whole-cell capacitance and series resistance. Before recording, cells were lifted up from the coverslip to facilitate solution exchange. Currents were recorded at a sampling rate of 2 kHz or greater, filtered at 1 kHz, and digitized using Clampex version 8.0 software (Molecular Devices).

Application of agonist solutions. Solutions containing agonist were applied to whole cells or outside-out patches using a piezo motor-driven 2 × 2 glass capillary tube capable of rapidly switching among up to four different solutions, as described previously (Forman, 1999). Agonist solutions were made in glass beakers, drawn up into glass syringes, and delivered to the perfusion device via polytetrafluoroethylene tubing (Cole-Parmer, Vernon Hills, IL) using a Physio 22 syringe pump (Harvard Apparatus, Holliston, MA) set to a flow rate of 4 ml/h per lumen. The open-tip solution exchange rate was 4600 ± 1100 s⁻¹ (n = 11) as determined by rapidly switching between 25 and 100 mM KCl at a holding potential of 0 mV.

During the first several minutes after achieving the whole-cell configuration, a variable amount of current rundown, as well as an increase in

the desensitization rate, was typically observed. However, the morphology of current traces stabilized after 5–10 min. Therefore, before data acquisition, 1 s pulses of 100 μM 5-HT were applied every 60 s to all new cells, until two to three consistent current traces with the same peak current amplitudes and desensitization kinetics were observed.

Curve fitting and data analysis. All data were fit to exponential equations using the Levenberg–Marquardt method in Clampfit version 9.2 (Molecular Devices). With prolonged applications of lower concentrations of 5-HT (<10 μM) and all concentrations of DA, current traces were fit to a double-exponential equation from a point past the initial inflection point of current activation to a point at which 90% of the current had decayed back to baseline. This approach simultaneously yielded both the activation rate and the desensitization rate. At higher concentrations of 5-HT at which activation and desensitization occurred on vastly different timescales, this approach often failed. Therefore, the rates of activation and desensitization were determined separately. To obtain the activation rate, current traces were fit to a double-exponential equation beginning from a point immediately after the initial inflection point of activation and ending at a point at which 5–10% of the current had decayed. The rate of the negative amplitude component was taken as the activation rate. To obtain the desensitization rate, traces were fit to a single-exponential equation beginning at the point at which 5% of the current had decayed and ending when 90% of the current had decayed.

The rate of current decay on termination of 5-HT (i.e., deactivation) was determined by fitting traces to a single-exponential equation from the start of current decay to a point at which 90% of the current had decayed toward baseline. The complex rate of current decay on termination of DA was quantified as the 90–10% decay time reported by Clampfit.

Each data point represents the mean ± SD value determined using three to five different cells. Concentration–response curves were fit to either a Hill equation or an exponential equation using Igor Pro version 4.01 (WaveMetrics, Lake Oswego, OR). Statistical analysis (*t* test) was performed using Prism version 4.01 (GraphPad Software, San Diego, CA).

Kinetic modeling. Simulated macroscopic current traces were generated with Channelab version 2.030526 (Synaptosoft, Decatur, GA) using a fifth-order Runga–Kutta algorithm and analyzed in Clampfit using the approach described above for electrophysiological macroscopic current traces. The simulated time courses for resensitization and recovery after activation were generated by approximating the initial probabilities for the A₃D and A₃O states, respectively, as unity and monitoring the time-dependent change in the fraction of receptors in resting and open states in the absence of agonist.

Results

Assessment of buffer solution exchange times

Several sets of experiments were used to assess our whole-cell solution exchange rate to ensure that it was sufficient to define 5-HT_{3A} receptor kinetics. First, we compared the activation rates of whole-cell currents mediated by human 5-HT_{3A} receptors transiently expressed in HEK293 cells with those mediated by human α1β2γ2 GABA_A receptors stably expressed in HEK293 cells; GABA_A receptors gate relatively quickly (Maconochie et al., 1994) and therefore are useful tools for assessing whole-cell solution exchange rates. When 1 mM GABA was applied to HEK293 cells expressing GABA_A receptors, currents activated at a rate of 1860 ± 420 s⁻¹. In comparison, when an equal concentration of 5-HT was applied to HEK293 cells expressing 5-HT_{3A} receptors, currents activated at a rate of 400 ± 120 s⁻¹. In analogous experiments, we measured activation rates in cells that stably expressed GABA_A receptors and were transiently transfected with cDNA encoding the 5-HT_{3A} subunit. These cells simultaneously expressed both receptor types, allowing the activation rates of GABA_A and 5-HT_{3A} receptors to be compared in the same cell. Figure 1A shows a representative pair of current traces recorded from one such cell when activated by either 5-HT or GABA (both

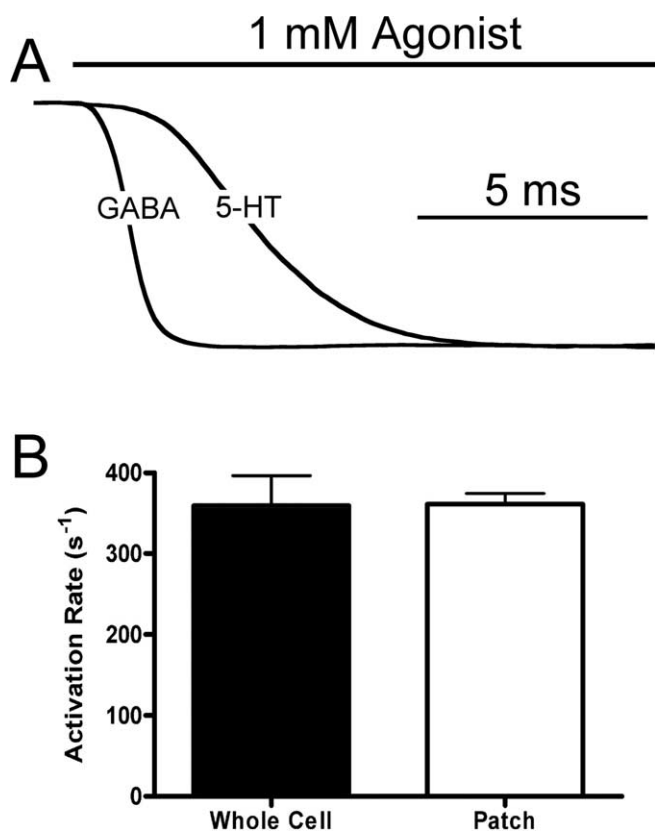


Figure 1. Whole-cell solution exchange time does not limit the measurement of 5-HT_{3A} receptor activation rates. **A**, Representative pair of traces obtained from a single whole HEK293 cell expressing both 5-HT_{3A} and α 1 β 2 γ 2 GABA_A receptors. Currents were activated with either 1 mM 5-HT or 1 mM GABA and normalized to the same peak amplitude. **B**, Summary data of receptor activation rates obtained from whole HEK293 cells expressing 5-HT_{3A} receptors (left) or outside-out patches pulled from HEK293 cells expressing 5-HT_{3A} receptors (right). 5-HT_{3A} receptor currents were activated with 100 μ M 5-HT. Each bar represents the mean \pm SD. The average activation rates of 5-HT_{3A} receptors in whole cells versus patches were identical (380 \pm 80 vs 380 \pm 30 s⁻¹, respectively).

at 1 mM) in the whole-cell configuration. The average rates of current activation in these cells ($n = 2$) were 547 s⁻¹ for 5-HT and 1976 s⁻¹ for GABA. Because 5-HT_{3A} receptors activated consistently more slowly than GABA_A receptors in whole HEK293 cells, we conclude that the rate of 5-HT_{3A} receptor activation was not limited by the speed of whole-cell solution exchange. As an additional test of the adequacy of our whole-cell solution exchange rate to quantify 5-HT_{3A} receptor activation kinetics, we measured the activation rate of 5-HT_{3A} receptors obtained from outside-out patches pulled from HEK293 cells expressing 5-HT_{3A} receptors and compared it with that determined using whole cells (100 μ M 5-HT). In the case of patches, we expect our solution exchange rate to approach our open-tip solution exchange rate (4600 \pm 1100 s⁻¹). The activation rate using patches was 360 \pm 30 s⁻¹ (Fig. 1B), identical to that measured using whole cells (360 \pm 80 s⁻¹) and well below the open-tip solution exchange rate. These results further support our conclusion that the speed of whole-cell solution exchange does not limit our measurements of 5-HT_{3A} receptor activation.

Activation of human 5-HT_{3A} receptors

For both 5-HT and DA, the peak agonist-evoked current amplitude increased steeply with agonist concentration before reaching a plateau (Fig. 2A). For 5-HT activated currents, a fit of the

peak current amplitude as a function of agonist concentration to a Hill equation gave an EC₅₀ of 2.7 \pm 0.2 μ M and a Hill coefficient of 1.8 \pm 0.2. For DA activated currents, the EC₅₀ was 195 \pm 16 μ M and the Hill coefficient was 2.3 \pm 0.3. In addition, the peak amplitudes of currents evoked by high concentrations of DA were only 15.7 \pm 0.4% of those evoked by high concentrations of 5-HT. This is consistent with previous studies using 5-HT_{3A} receptors expressed in *Xenopus* oocytes, indicating that DA is a partial agonist of 5-HT_{3A} receptors (Lovinger et al., 2000; Solt et al., 2005).

At intermediate 5-HT concentrations (2–100 μ M), the activation rate increased with 5-HT concentration, indicating that receptor activation was rate limited by agonist binding kinetics (Fig. 2B). At high 5-HT concentrations (>100 μ M) in which channel gating (rather than agonist binding) kinetics are expected to limit the rate of activation, the activation rate reached a plateau equal to 400 \pm 80 s⁻¹. At low 5-HT concentrations (\leq 2 μ M), the activation rate also began to plateau, reaching 1.4 \pm 0.6 s⁻¹ at 0.3 μ M.

In contrast, the activation rate evoked by DA varied little over the entire concentration range studied (30 μ M to 2 mM) and averaged 3.1 \pm 1.6 s⁻¹. This suggests that, throughout this DA concentration range, activation rates are limited by channel gating rather than agonist binding kinetics. We could not analyze currents evoked by concentrations of DA lower than 30 μ M, at which we expected activation rates to be rate limited by agonist binding kinetics because currents were too small.

Desensitization of human 5-HT_{3A} receptors

After activation, currents decayed to baseline with the continuous application of agonist, reflecting the process of desensitization. Although we estimate that we would have detected steady-state currents evoked by long (87 s) pulses of 100 μ M 5-HT had they been at least 1% of the peak current response, no such currents were observed. Similarly, any steady-state current present on equilibration with 1 mM DA was too small to measure (data not shown). Desensitization on application of 5-HT or DA followed a single-exponential time course over at least 90% of the current decay (Fig. 3A). Figure 3B shows the agonist concentration dependence of the rate of desensitization. For both 5-HT and DA, the rate of desensitization increased with agonist concentration before reaching a plateau equal to 1.15 \pm 0.07 s⁻¹ for 5-HT and 0.25 \pm 0.07 s⁻¹ for DA. A fit of the data to a Hill equation yielded EC₅₀ values of 3.6 \pm 0.6 μ M for 5-HT and 400 \pm 260 μ M for DA, similar to their respective EC₅₀ values for peak current activation and respective Hill coefficients of 3 \pm 1.8 and 1.4 \pm 0.9.

The rate of resensitization after 5-HT-induced desensitization was assessed using a double agonist pulse protocol (Fig. 4A). In each experiment, 100 μ M 5-HT was continuously applied for 15 s to desensitize receptors. After a variable recovery period (1–30 s) during which receptors were exposed to buffer only, 100 μ M 5-HT was reapplied for 1 s to assess the fraction of receptors that could be activated. A 60 s recovery period was used between experiments to allow complete resensitization. The rate of resensitization was assessed as the recovery time dependence of the peak current amplitude evoked by the second 5-HT pulse normalized to that evoked by the first 5-HT pulse. The rate of resensitization after DA-induced desensitization was assessed using a similar approach. We first defined the peak current response to a 1 s pulse of 100 μ M 5-HT. After a 60 s recovery period in buffer, 1 mM DA was continuously applied for 50 s to induce full desensitization. After a variable recovery time (0.05–10 s) during which

receptors were exposed to buffer only, 100 μM 5-HT was reapplied for 1 s. The rate of resensitization from DA-induced desensitization was then assessed from the time dependence of the peak current response evoked by the second 5-HT pulse normalized to that evoked by the first 5-HT pulse. Figure 4B compares the time course of resensitization when desensitization was induced by 5-HT versus DA. In the case of 5-HT, the time course of resensitization was sigmoidal, suggestive of a multistep recovery mechanism. The mean data were fit to the Hodgkin–Huxley equation: $I_t = (I_{\text{max}}^{1/m} - (I_{\text{max}}^{1/m} - I_0^{1/m})\exp(-t/\tau))^m$, where I_t is the normalized peak current at a given recovery time, I_{max} is the normalized peak current with long recovery times, I_0 is the current at time 0 (i.e., the steady-state desensitized current), τ is the recovery time constant, and m approximates the number of equivalent rate-limiting steps along the route of recovery (Robert and Howe, 2003). Because no steady-state desensitized current could be measured, I_0 was fixed at zero. The value of m was 3.8 ± 0.1 , suggesting that there are three or four equivalent rate-limiting steps along the recovery pathway, τ was 4.83 ± 0.07 s, and I_{max} was 0.936 ± 0.003 .

The time course of resensitization after DA-induced desensitization was not sigmoidal and occurred more quickly than after 5-HT-induced desensitization, with 50% recovery requiring ~ 1 s. A fit of the DA data to the Hodgkin–Huxley equation yielded values of 0.79 ± 0.01 , 1.4 ± 0.3 s, and 0.87 ± 0.03 for m , τ , and I_{max} , respectively.

Deactivation of human 5-HT_{3A} receptors

To measure the rate of receptor deactivation, an agonist pulse ranging in duration from 3 ms (for high 5-HT concentrations) to several seconds (for low 5-HT concentrations and all DA concentrations) was applied to whole cells expressing 5-HT_{3A} receptors. The goal was to achieve a sufficient peak current response to accurately measure the deactivation rate while minimizing the impact of desensitization during the agonist pulse. On termination of the agonist pulse, current amplitudes decayed. For 5-HT, this decay followed an exponential time course over at least 90% of its amplitude, and its rate varied little with 5-HT concentration (1–100 μM), ranging from 0.76 ± 0.14 to 2.3 ± 0.4 and averaging 1.3 ± 0.6 s⁻¹ (Fig. 5A,B). This rate was similar to the rate of desensitization induced by high 5-HT concentrations. For DA, the current decay was faster and complex as reflected by our consistent inability to achieve satisfactory fits of the current decay to multiexponential equations having fewer than four components. Therefore, we quantified the kinetics of this process as the 90–10% decay time (Fig. 5C). Figure 5D shows that this decay time varied little with DA concentration (100 μM to 2 mM), ranging from 0.17 ± 0.02 to $0.29 \pm 0.30 \pm 0.09$ s and averaging 0.23 ± 0.05 s.

To determine whether receptors activated by 5-HT would reopen after deactivation, we activated receptors with a brief (5–10 ms) pulse of 100 μM 5-HT and, after a variable recovery period (1–30 s) in buffer, reapplied 100 μM 5-HT for 1 s. We then compared the amplitude of the current evoked by the second agonist

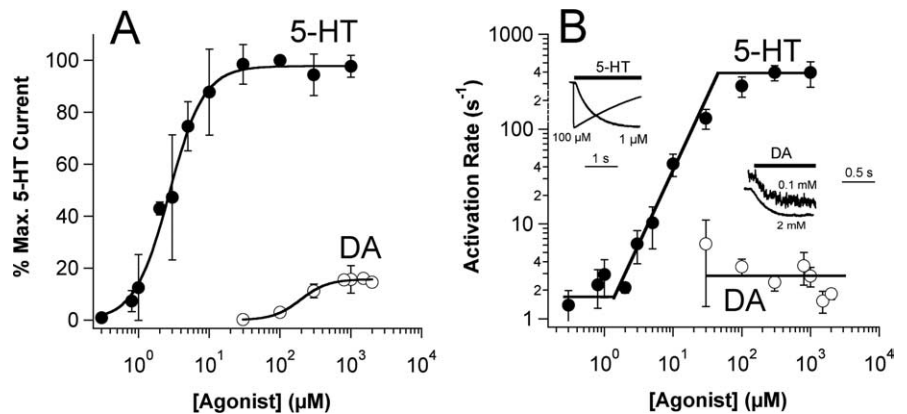


Figure 2. Relationship between the agonist concentration and the peak current response (**A**) or rate of activation (**B**). **A**, Agonist concentration–response curves for peak current activation. Responses were normalized to the peak current evoked by 100 μM 5-HT in the same cell. The two curved lines are fits of the 5-HT and DA datasets to a Hill equation, and the results of the fits are given in Results. **B**, Agonist concentration–response curves for the rate of activation. In the 5-HT dataset, the three lines were drawn by eye to illustrate the low (≤ 2 μM) and high (> 100 μM) 5-HT concentration asymptotes and the agonist dependence of the activation rate at intermediate (2–100 μM) 5-HT concentrations. In the DA dataset, the line indicates the average activation rate across all DA concentrations. Examples of current traces evoked by either 1 or 100 μM 5-HT or 0.1 or 2 mM DA are shown as insets. The DA traces were offset from one another to facilitate comparison. In both panels, each data point represents the mean \pm SD.

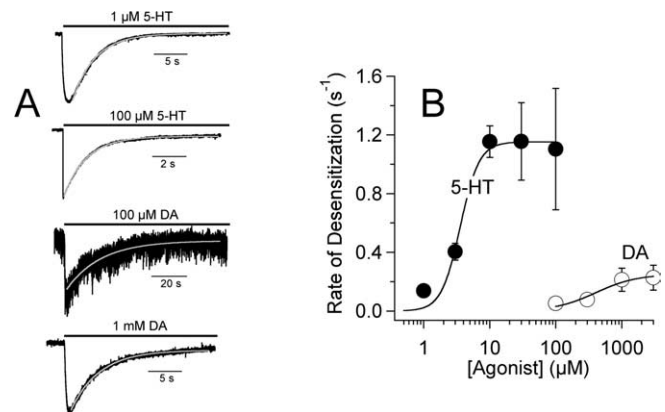


Figure 3. Relationship between the agonist concentration and the desensitization rate. **A**, Representative current traces recorded on the rapid and continuous application of (from top to bottom) 1 μM 5-HT, 100 μM 5-HT, 100 μM DA, and 1 mM DA to HEK293 cells expressing 5-HT_{3A} receptors. Single-exponential fits of the desensitization process are superimposed on current traces as gray curves to demonstrate that desensitization closely approximates a single-exponential process. **B**, Agonist concentration dependence of the rate of desensitization. Each data point represents the mean \pm SD. The two curved lines are fits of the 5-HT and DA datasets to a Hill equation, and results of the fits are given in Results.

pulse with that evoked by the first. A 60 s recovery period was used between each set of agonist pulses to allow complete resensitization between each experiment. Figure 6 shows that, even several seconds after the first brief agonist pulse, many receptors could not be reactivated because the peak current amplitude of the second agonist pulse was considerably smaller than that of the first one. However, the response to the second agonist pulse increased with longer recovery times. A plot of the amplitude ratio versus recovery time was biphasic and, when fit to a double-exponential equation, yielded rates of 1.2 ± 0.09 and 0.09 ± 0.01 s⁻¹ for the decreasing and increasing phases, respectively, with amplitudes of 0.89 ± 0.03 and 0.91 ± 0.022 .

Kinetic mechanism of human 5-HT_{3A} receptor function

To interpret our data and better understand the differences in receptor function produced by these two agonists, we analyzed

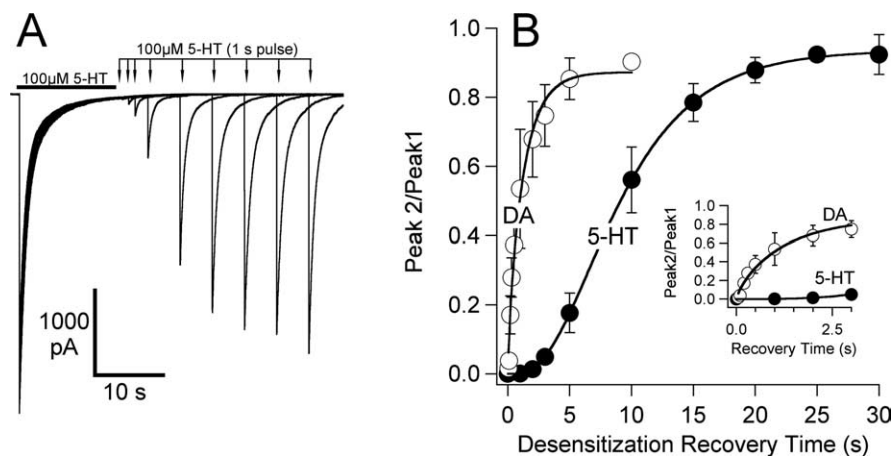


Figure 4. Resensitization of human 5-HT_{3A} receptors. **A**, Representative series of nine pairs of current traces obtained from the same cell expressing 5-HT_{3A} receptors using different desensitization recovery times. Cells were perfused with 100 μ M 5-HT for 15 s. After a recovery time ranging from 1 to 30 s, a second test pulse of 100 μ M 5-HT was applied for 1 s. **B**, Recovery time dependence of the peak response to the second 5-HT pulse normalized to the peak response of the first 5-HT pulse. Desensitization was induced by prolonged exposure of receptors to either 5-HT or DA. The inset shows the first 3 s on an expanded timescale. Each data point represents the mean \pm SD. The solid curves are single-exponential fits of the 5-HT and DA datasets. The two curved lines are fits of the 5-HT and DA datasets to the Hodgkin–Huxley equation. For 5-HT, I_{max} , m , and τ were 0.936 ± 0.003 , 3.8 ± 0.1 , and 4.83 ± 0.07 s, respectively. For DA, these values were 0.87 ± 0.03 , 0.79 ± 0.1 , and 1.4 ± 0.3 s, respectively.

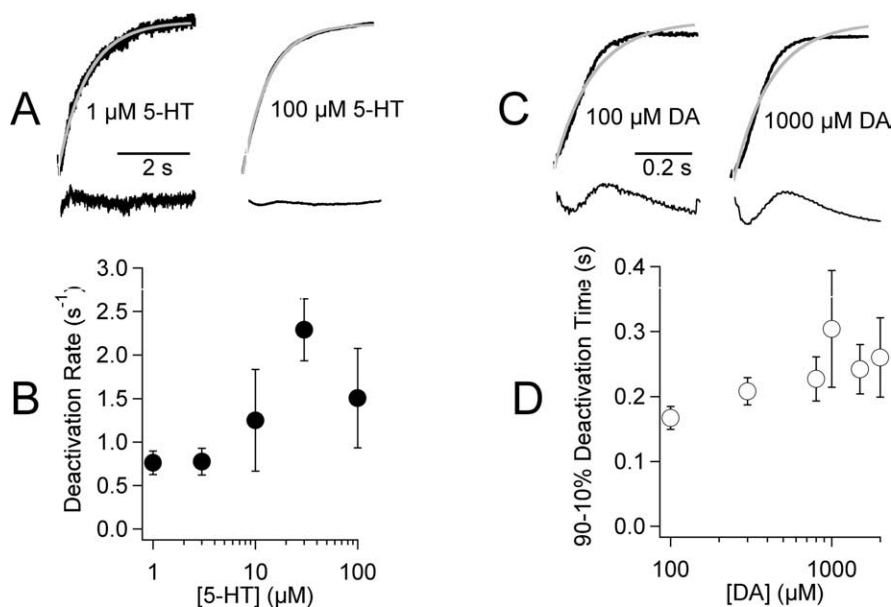


Figure 5. Deactivation of human 5-HT_{3A} receptors. **A**, Representative traces showing deactivation after activation by 1 or 100 μ M 5-HT. Single-exponential fits of the deactivation process are superimposed on current traces as gray curves. The residuals from each fit are shown below each current trace. **B**, 5-HT concentration dependence of the rate of deactivation. Each data point represents the mean \pm SD. The average rate of deactivation across all 5-HT concentrations was 1.3 ± 0.6 s⁻¹. **C**, Representative traces showing deactivation after activation by 100 μ M or 1 mM DA. Single-exponential fits of the deactivation process are superimposed on current traces as gray curves. The residuals from each fit are shown below each current trace. Note that fitting deactivation after activation by DA to a single exponential produced poor results. **D**, DA concentration dependence of the rate of deactivation. Each data point represents mean \pm SD. Because single-exponential fits were poor, the rate of deactivation was quantified as the 90–10% decay time. Across all DA concentrations, this deactivation time averaged 0.23 ± 0.05 s.

our data within the context of a cyclic allosteric model (Fig. 7) that is analogous to those used for other members of the Cys-loop superfamily of ligand-gated ion channels (Changeux and Edelman, 2001; Grosman and Auerbach, 2001; Rusch et al., 2004). In such models, receptors are considered to exist in equilibria among three states: resting (R), open (O), and desensitized (D). The resting state predominates in the absence of agonist, but

agonist binding shifts the receptor population toward open and desensitized states that have higher agonist affinity. Because each 5-HT_{3A} receptor consists of five identical subunits, it can theoretically bind as many as five agonist molecules. However, the Hill coefficient for peak current activation is ~ 2 , suggesting that maximal gating efficacy is achieved when two or three sites are occupied. Electrophysiological and kinetic modeling studies of murine 5-HT_{3A} receptors suggest that the binding of at least three agonist molecules is required to open channels (Mott et al., 2001). Studies of two other structurally related homopentameric Cys-loop receptors (the $\alpha 1$ glycine and $\rho 1$ GABA receptors) suggest that maximal gating efficacy occurs when three agonist molecules are bound (Chang and Weiss, 1999b; Beato et al., 2004; Yang et al., 2006). Therefore, by analogy to these receptors, we assumed that 5-HT_{3A} receptor gating occurs when three agonist binding sites are occupied. To simplify our model and provide constraints, we made several additional assumptions. First, we assumed that all of the agonist binding sites on each state are equal and independent (i.e., no cooperativity in binding). Second, we assumed that the agonist association rates (k_1) for all states are equal. Third, we assumed that the agonist affinities of open and desensitized receptors are the same. Fourth, we assumed that the conductances of all open states are equal. Fifth, we assumed that the rate constants for desensitization for both agonists are equal, because we could not characterize the rate of DA binding to the resting state, we assumed that the association rate constant for DA is the same as that determined for 5-HT.

For each agonist, the value of each kinetic parameter was estimated from the mean datasets shown in previous figures. When possible, the value was derived by fitting the relationship between mean data and either agonist concentration or recovery time. For example, the value of k_{d+} for 5-HT was taken as the maximum rate of desensitization determined by fitting the relationship between the rate of desensitization and the 5-HT concentration to a Hill equation. Similarly, k_3 (for 5-HT) and k_{DR} (for DA) were defined as the inverse time constant determined by fitting the relationship between the rate of resensitization and the recovery time to the Hodgkin–Huxley equation. Kinetic parameters that could not be derived directly by fitting were estimated by trial and error to produce simulated datasets that visually matched the experimental datasets. For example, the agonist association and dissociation rate constants k_1 and k_2 were estimated from both the 5-HT concentration dependence of the activation rate at in-

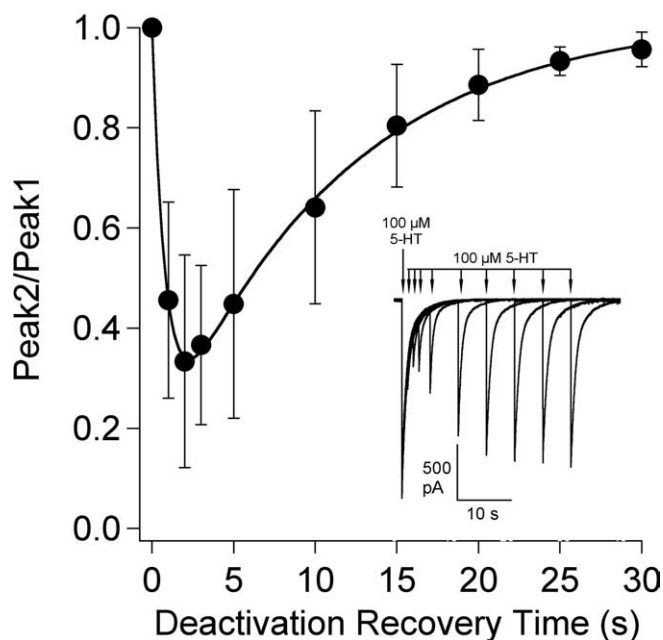


Figure 6. Recovery from deactivation after activation by 5-HT. Inset shows a series of nine pairs of current traces obtained from the same representative cell expressing 5-HT_{3A} receptors using different deactivation recovery times. Cells were perfused with 100 μ M 5-HT for 5–10 ms, and, after a recovery period ranging from 1 to 30 s, a second pulse of 100 μ M 5-HT was applied for 1 s. The plot shows the biphasic recovery time dependence of the response to the second 5-HT pulse normalized to the response to the first 5-HT pulse. Each data point represents the mean \pm SD. The curve is a fit of the dataset to a double-exponential equation, which yielded rates of 1.2 ± 0.09 and 0.09 ± 0.01 s⁻¹ for the decreasing and increasing phases, respectively.

intermediate concentrations and the low 5-HT concentration asymptote of the activation rate.

Table 1 lists the values of the kinetic parameters defined by our model for 5-HT and DA to simulate our data. It is important to note that the agonist binding rates are the products of the association rate constant (k_1) and a statistical factor that reflects the number of available agonist binding sites. Initially, all five sites can bind agonist, and, therefore, the binding rate of the first step is defined as $5k_1$. However, the binding rates of subsequent agonist molecules are reduced in proportion to the number of occupied agonist binding sites. Similarly, the agonist unbinding rate depends not only the dissociation rate constant (k_2 or k_3) but also on the number of agonist molecules bound to the receptor.

Modeling of 5-HT action on 5-HT_{3A} receptors

The inset in Figure 8A shows computer-simulated current traces obtained using our model and the parameters listed in Table 1 for 5-HT. A also plots the relationship between the 5-HT concentration and the peak current response of simulated traces. In this panel (and all others in this figure and in Fig. 9), the results of computer simulations are shown as lines or curves. For comparison, analogous data obtained from electrophysiological experiments are plotted as circles. The peak amplitude of the simulated current increased with 5-HT concentration before reaching a plateau. A fit of the peak amplitude of simulated traces versus 5-HT concentration to a Hill equation gave an EC₅₀ of 2.7 μ M and a Hill coefficient of 1.8 (fit not shown).

At intermediate 5-HT concentrations, the activation rate of simulated traces increased with 5-HT concentration, and our modeling confirmed that the relationship between the activation rate and the 5-HT concentration was dependent on the agonist association and dissociation rate constants k_1 and k_2 , respectively

(Fig. 8B). At high 5-HT concentrations, the activation rate of simulated traces reached a plateau value of 400 s⁻¹. Provided that desensitization is negligible on the timescale of channel gating, this rate equals the sum of the channel opening and closing rates, $\beta + \alpha$, in our model. For a highly efficacious agonist such as 5-HT, this maximal activation rate approximates β . Consequently, the value of β in our model was taken as this maximal activation rate. The activation rate of simulated traces also reached a minimum value of 1.5 s⁻¹ at low 5-HT concentrations, a value that our modeling indicated was highly dependent on the rates of channel closing and agonist unbinding but not on the rates of channel opening or agonist binding.

The rate of desensitization of simulated traces increased before reaching a plateau at high 5-HT concentrations of 1.15 s⁻¹ (Fig. 8C). Within the context of our model, the rate of desensitization at high 5-HT concentrations approximates the sum of the forward and backward rate constants for desensitization, $k_{d+} + k_{d-}$. In addition, the ratio between the steady-state current amplitude in the continued presence of a high concentration of 5-HT and the peak current amplitude evoked by a high 5-HT concentration approximates the ratio k_{d-}/k_{d+} . Because this ratio is <1%, we place the upper limit of k_{d-} at 0.01 s⁻¹, a rate so slow that the A₃D \rightarrow A₃O transition may be ignored without significantly affecting the behavior of the model, and the value of k_{d+} approximates the maximal rate of desensitization at high 5-HT concentrations (1.15 s⁻¹). A fit of the rate of desensitization of simulated traces versus 5-HT concentration to a Hill equation yielded an EC₅₀ of 1.7 μ M and a Hill coefficient of 3.3 (fit not shown).

During washout of 5-HT, our model predicted the sigmoidal resensitization time course (Fig. 8D). According to our model, this occurs because nearly all desensitized receptors are in the A₃D state and must unbind all three of their 5-HT molecules before returning to the resting state via the multistep pathway A₃D \rightarrow A₂D \rightarrow AD \rightarrow D \rightarrow R. The presence of three rate-limiting agonist unbinding steps in this pathway generally agrees with the number estimated using the Hodgkin–Huxley equation in which m was calculated as 3.8 ± 0.1 . When 5-HT dissociation from the desensitized state, rather than receptor isomerization from D to R, are the rate-limiting steps leading to resensitization, k_3 approximates the inverse of the recovery time constant determined using the Hodgkin–Huxley equation (0.207 ± 0.003 s⁻¹).

An important implication of our cyclic model is that, once a receptor reaches the predominant open state (i.e., A₃O), it may deactivate on termination of the agonist pulse via one of three pathways: (1) by returning to the preopen state (i.e., A₃R); (2) by unbinding ligand and then closing via the pathway A₃O \rightarrow A₂O \rightarrow AO \rightarrow O \rightarrow R; or (3) by desensitizing (proceeding to A₃D). Mainly because 5-HT k_{d+} is similar in magnitude to α and greater than k_3 , many open state receptors are predicted by our model to desensitize before they can return to the preopen state or unbind ligand on termination of even the briefest 5-HT pulse. In addition, some open state receptors that return to the preopen state on termination of 5-HT may reopen and then desensitize before they unbind 5-HT. This provides a simple explanation for why the rate of deactivation is similar to the rate constant for desensitization: a significant fraction of receptors desensitize during the deactivation process. This process is predicted by our model to have a rate that is 5-HT concentration independent (Fig. 8E) because, during deactivation, it occurs in the absence of free-agonist. Figure 8F demonstrates that the simulated time course for deactivation recovery, like the experimental data, is biphasic. According to our model, this occurs because many open

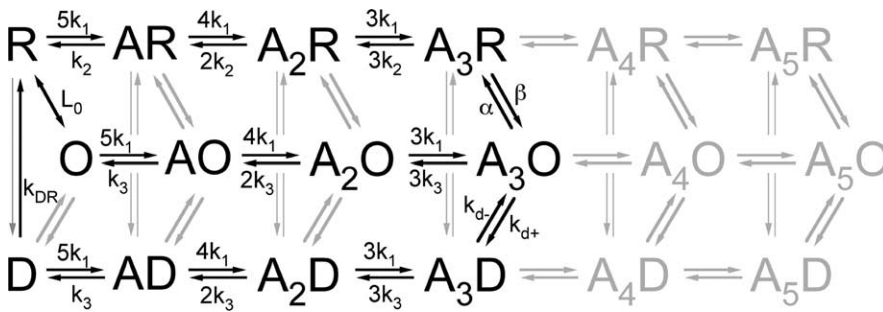


Figure 7. Kinetic scheme describing human 5-HT_{3A} receptor function. Major states and transitions required to account for the actions of 5-HT and DA on human 5-HT_{3A} receptors are shown in black. Minor states and transitions (shown in gray) were not included in simulations. L_0 defines the preexisting ratio $[R]/[O]$. The values of the kinetic parameters for 5-HT and DA are listed in Table 1.

Table 1. Rate and equilibrium constants for the human 5-HT_{3A} receptor model for 5-HT and DA

Kinetic parameter	5-HT	DA
k_1	$1 \times 10^7 \text{ M}^{-1} \text{ s}^{-1}$	$1 \times 10^7 \text{ M}^{-1} \text{ s}^{-1}$
k_2	200 s^{-1}	1700 s^{-1}
k_3	0.207 s^{-1}	14 s^{-1}
β	400 s^{-1}	0.6 s^{-1}
α	1 s^{-1}	1.2 s^{-1}
k_{d+}	1.15 s^{-1}	1.15 s^{-1}
k_{d-}	$<0.01 \text{ s}^{-1}$	$<0.01 \text{ s}^{-1}$
k_{DR}	0.7 s^{-1}	0.7 s^{-1}
L_0	3×10^6	3×10^6

Kinetic parameters for the model were constrained by the electrophysiological data presented in the figures or thermodynamic law. The value of k_{d-} is an upper limit estimate based on the inability to measure steady-state currents after equilibration with 100 μM 5-HT or 1 mM DA.

state receptors desensitize during the first few seconds of deactivation after even a brief 5-HT pulse, reducing the response to the second 5-HT pulse. However, with progressively longer recovery times that allow significant numbers of desensitized receptors to return to the resting state, the response to the second 5-HT pulse increases.

Modeling of DA action on human 5-HT_{3A} receptors

The left inset in Figure 9A shows computer-simulated current traces obtained using our model and the parameters for DA listed in Table 1. A also plots the relationship between the DA concentration and the peak current response of simulated traces. The peak amplitude of simulated currents increased with DA concentration before reaching a plateau. A fit of the peak amplitude of simulated traces versus DA concentration to a Hill equation gave an EC_{50} of $183 \pm 6 \mu\text{M}$, a Hill coefficient of 1.55 ± 0.06 , and a maximum amplitude at high concentrations that was $16.9 \pm 0.2\%$ of that evoked by high concentrations of 5-HT (fit not shown). Our modeling revealed that this maximum amplitude is significantly less than the 33% expected based on the channel-gating efficacy alone $[\beta/(\alpha + \beta)]$ by DA because channel gating and desensitization occur on similar timescales. Consequently, approximately one-half of all receptors have already reached the desensitized state by the time the peak current has been achieved. This truncates the peak current amplitude (Fig. 9A, right inset). Figure 9B demonstrates that the activation rates of simulated DA-evoked currents did not vary significantly with concentrations of DA concentrations ranging from 30 μM to 2 mM and averaged $2.7 \pm 0.1 \text{ s}^{-1}$, within the range obtained with electrophysiological studies ($3.1 \pm 1.6 \text{ s}^{-1}$). The rate of desensitization of simulated traces increased before reaching a plateau at high DA

concentrations (Fig. 9C). A fit of a plot of the desensitization rate of simulated traces versus DA concentration to a Hill equation yielded an EC_{50} of $218 \pm 7 \mu\text{M}$, a Hill coefficient of 1.5 ± 0.1 , and a maximum value of $0.244 \pm 0.002 \text{ s}^{-1}$ at high DA concentrations (fit not shown).

After desensitization by DA, our model predicted the experimental observation that resensitization occurs without a sigmoidal time course because DA, unlike 5-HT, dissociates from desensitized receptors within tens of milliseconds, and the rate-limiting step for resensitization is simply the $D \rightarrow R$ transition (Fig. 9D). A single rate-limiting step for DA resensitization is consistent with the number estimated using the Hodgkin–Huxley equation in which m was calculated to be 0.79 ± 0.1 . The rate constant defining this transition was estimated as the inverse of the recovery time constant determined using this equation ($0.7 \pm 0.2 \text{ s}^{-1}$).

After activation by DA, our model predicted the experimental observation that deactivation is faster than either activation or desensitization and follows a complex time course. Because k_3 for DA is an order of magnitude faster than either α or k_{d+} , nearly all receptors opened by DA deactivate by first unbinding all agonist molecules and then closing via the pathway $A_3O \rightarrow A_2O \rightarrow AO \rightarrow O \rightarrow R$. Our modeling demonstrated that the current decay resulting from such deactivation is complex because it involves sequential increases and decreases in the concentrations of open states A_2O , AO , and O as DA dissociates from open state receptors before channel closure (Fig. 9E). One subtle difference between simulated and experimental deactivation traces is that, although the time courses of both are complex, the sigmoidal lag immediately after that agonist termination was less pronounced in experimental traces. Our modeling indicated that this could result from small differences in the conductances of open states having different numbers of agonist molecules bound. After termination of a 3 s pulse of DA, the 90–10% decay time of simulated current traces was DA concentration independent and equal to 0.22 s (Fig. 9F), in agreement with the value of 0.23 ± 0.05 determined in electrophysiological experiments.

After activation by DA, our model predicted the experimental observation that deactivation is faster than either activation or desensitization and follows a complex time course. Because k_3 for DA is an order of magnitude faster than either α or k_{d+} , nearly all receptors opened by DA deactivate by first unbinding all agonist molecules and then closing via the pathway $A_3O \rightarrow A_2O \rightarrow AO \rightarrow O \rightarrow R$. Our modeling demonstrated that the current decay resulting from such deactivation is complex because it involves sequential increases and decreases in the concentrations of open states A_2O , AO , and O as DA dissociates from open state receptors before channel closure (Fig. 9E). One subtle difference between simulated and experimental deactivation traces is that, although the time courses of both are complex, the sigmoidal lag immediately after that agonist termination was less pronounced in experimental traces. Our modeling indicated that this could result from small differences in the conductances of open states having different numbers of agonist molecules bound. After termination of a 3 s pulse of DA, the 90–10% decay time of simulated current traces was DA concentration independent and equal to 0.22 s (Fig. 9F), in agreement with the value of 0.23 ± 0.05 determined in electrophysiological experiments.

Discussion

The present studies demonstrate that the rates of human 5-HT_{3A} receptor activation, deactivation, desensitization, and resensitization are considerably different when induced by the high-efficacy agonist 5-HT versus the low-efficacy agonist DA. Within the context of an allosteric kinetic model of 5-HT_{3A} receptor function, the differences between the two agonists are primarily attributable to the very different rates with which they induce channel opening (β) and dissociate from open and desensitized receptor states (k_3).

Our electrophysiological and kinetic modeling studies also revealed several interesting characteristics of human 5-HT_{3A} receptor function. First, 5-HT_{3A} receptors open very slowly relative to other Cys-loop receptors with channel opening rate constants estimated to be 400 and 0.6 s^{-1} when receptors are activated by 5-HT and DA, respectively. For comparison, the opening rate constant of the nicotinic acetylcholine receptor has been estimated to be $60,000 \text{ s}^{-1}$ when activated by acetylcholine (Maconochie and Steinbach, 1998) and that of the GABA_A receptor is $\sim 6000 \text{ s}^{-1}$ when activated by GABA (Maconochie et al., 1994).

Second, 5-HT_{3A} receptors close relatively slowly. Consequently, other routes out of the open state besides the return to the preopen state contribute significantly to the deactivation process. In the case of 5-HT, the fastest route out of the open state is via desensitization (Fig. 10). Therefore, many open state receptors desensitize on termination of a 5-HT pulse regardless of the pulse duration. This explains why the rate of deactivation is comparable with the rate constant for desensitization and why recovery from deactivation and resensitization occur on similar timescales. The conclusion that desensitization contributes significantly to the deactivation process when 5-HT is the agonist may also explain why mutations in transmembrane-linking domains that alter the rate of 5-HT-induced desensitization produce parallel changes in the rate of deactivation (Hu and Lovinger, 2005; Hu et al., 2006). However, in the case of DA, deactivation occurs via a different route because DA dissociates from open states an order of magnitude faster than open states either return to the preopen state or desensitize. Therefore, nearly all open state receptors deactivate by first losing all of their DA molecules and then closing from the unliganded open state. Third, the agonist EC₅₀ values for channel activation and desensitization are similar. The most parsimonious explanation for this observation is that agonist-induced desensitization occurs primarily from the open state. Accordingly, at high concentrations, 5-HT induces desensitization more quickly than DA simply because a greater fraction of receptors reach the open state (i.e., 5-HT is a more efficacious agonist than DA) and not because its rate constant for desensitization is faster. Fourth, recovery from 5-HT-induced desensitization, but not DA-induced desensitization, occurs with sigmoidal time course. This occurs because recovery from 5-HT-induced desensitization is rate limited by the slow, sequential dissociation of three 5-HT molecules from high-affinity desensitized receptors. In the case of DA-induced desensitization, DA dissociates from desensitized receptors nearly two orders of magnitude faster than 5-HT, and the rate-limiting step leading to recovery is the D → R transition. Because of its more rapid dissociation rate, DA has a lower affinity for the desensitized (and open) state than 5-HT, consistent with previous studies showing that DA has a higher IC₅₀ than 5-HT for inducing 5-HT₃ receptor desensitization (van Hooff and Vijverberg, 1996).

The strategy we used for developing the model for 5-HT_{3A} receptor function is based on the symmetry allosterism principles first formalized by Monod, Wyman, and Changeux (MWC)

(Monod et al., 1965). Both equilibrium and kinetic MWC allosteric models for agonist binding, channel gating, and desensitization have been presented previously in studies of both nicotinic acetylcholine receptors (Edelstein et al., 1996; Changeux and

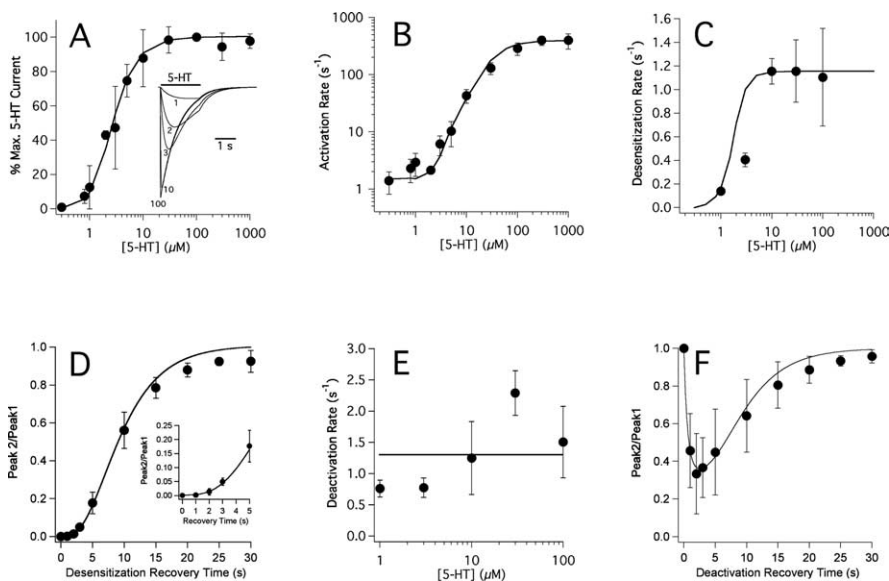


Figure 8. Modeling of 5-HT action on 5-HT_{3A} receptors. In all panels, the results of computer simulations are shown as lines or curves, and analogous data obtained from electrophysiological experiments are shown for comparison as circles ± SD. **A**, Relationship between the 5-HT concentration and the peak current response. The inset shows simulated current traces at the indicated 5-HT concentrations (micromolar). **B**, Relationship between the 5-HT concentration and the rate of activation. **C**, Relationship between the 5-HT concentration and the desensitization rate. **D**, Time course of recovery from 5-HT-induced desensitization. The inset shows the early time domain on an expanded scale. **E**, 5-HT concentration dependence of the rate of deactivation. **F**, Time course of recovery from deactivation after activation by 5-HT.

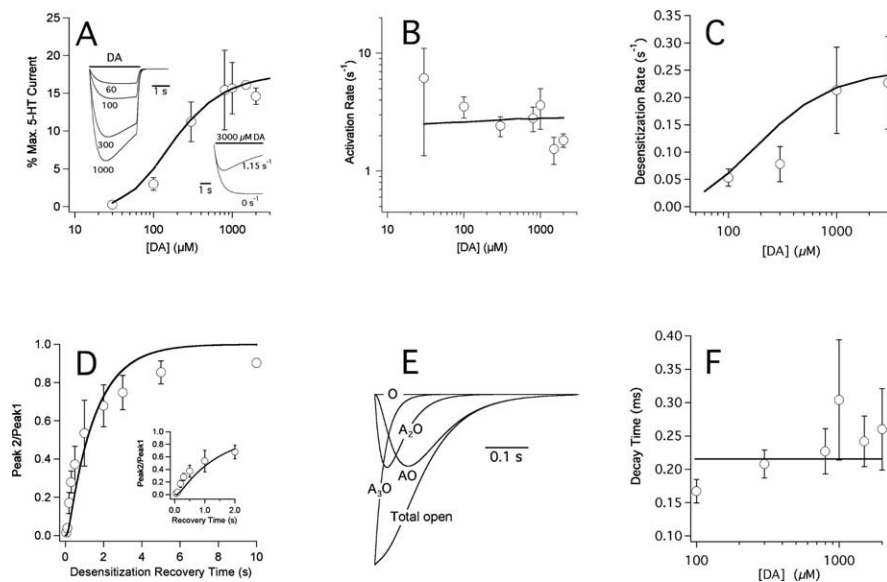


Figure 9. Modeling of DA action on 5-HT_{3A} receptors. In all panels, the results of computer simulations are shown as lines or curves, and analogous data obtained from electrophysiological experiments are shown for comparison as circles. **A**, Relationship between the DA concentration and the peak current response. The left inset shows simulated current traces at the indicated DA concentrations (micromolar). The right inset shows two simulated 3 mM DA-evoked current traces with k_{d+} equal to either 1.15 or 0 s⁻¹ (i.e., no desensitization). Note that desensitization significantly reduced the simulated peak current response. **B**, Relationship between the DA concentration and the rate of activation. **C**, Relationship between the DA concentration and the desensitization rate. **D**, Resensitization rate after DA-induced desensitization. The inset shows the first 2 s on an expanded scale. **E**, Simulations showing the relative current carried by each open state as a function of time on termination of a 3 s pulse of 1 mM DA. “Total open” is the sum of the currents carried by all open states and corresponds to the predicted current decay on deactivation. **F**, DA concentration dependence of the deactivation time.

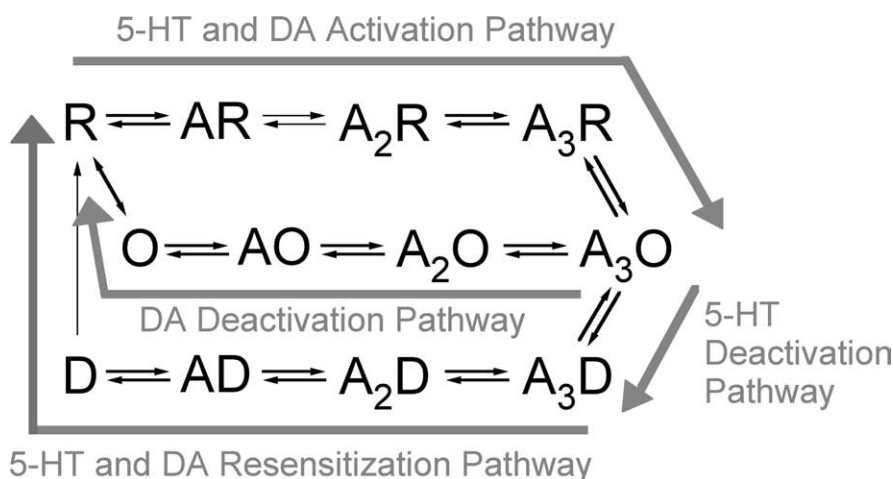


Figure 10. Predominant pathways of human 5-HT_{3A} receptor activation, deactivation, and resensitization. Activation by 5-HT and DA occurs via the same pathway, whereas deactivation occurs via different pathways. For 5-HT, currents decay during deactivation primarily because open state receptors isomerize to the desensitized state. For DA, currents decay during deactivation because open state receptors unbind DA molecules and then return to the resting state. For neither agonist is the predominant pathway for deactivation the reverse of the activation pathway. Resensitization after desensitization by either 5-HT or DA requires agonist unbinding, followed by $D \rightarrow R$ isomerization. Minor states and transitions have been omitted for clarity.

Edelstein, 2001) and GABA_A receptors (Chang and Weiss, 1998, 1999a; Chang et al., 2002; Scheller and Forman, 2002; Rusch et al., 2004; Rusch and Forman, 2005) but not 5HT_{3A} receptors. The majority of kinetic models for ligand-gated ion channels invoke sequential binding-gating schemes based on principles introduced by Koshland et al. (1966). Sequential models typically remove cyclic constraints and reduce the number of states needed when analyzing data. In contrast, MWC models usually contain many states but also impose equilibrium cyclic constraints that reduce the overall number of free parameters (Edelstein et al., 1996; Rusch et al., 2004).

The minimum allosteric model that we used to simulate the actions of 5-HT and DA on human 5-HT_{3A} receptors contains 12 states, nine rate constants, and one equilibrium constant. By definition, rate constants and equilibria between unliganded states are the same for 5-HT and DA, and, in the case of L_0 , was estimated to be $\sim 3 \times 10^6$ by cyclic thermodynamic constraints imposed by the values of other kinetic steps. For comparison, L_0 for the nicotinic acetylcholine and GABA_A receptors have been estimated to be 10^7 – 10^8 (Purohit and Grosman, 2006) and 10^4 – 10^5 (Chang and Weiss, 1999a; Rusch and Forman, 2005), respectively. There are additional minor states and transitions in our model that were not necessary for adequate simulation of our data. However, because some of these transitions also occur within cycles, we can calculate the associated equilibrium constants. For example, when 5-HT is the agonist, the open probability of single and double liganded receptors is calculated to be 4.3×10^{-4} and 0.41 respectively, compared with >0.99 for triple liganded receptors. Presumably, these transitions do not contribute significantly to receptor function because the underlying rate constants are slow relative to those between triple liganded states.

Although our minimum model assumes that gating occurs when three agonist binding sites are occupied, we also explored the possibility that gating could occur with either two or four sites occupied. For both 5-HT and DA, our modeling showed that, when gating occurs with two agonist binding sites occupied, the relationship between the peak current amplitude and the agonist concentration is too shallow (i.e., the Hill coefficient is too small) to account for our electrophysiological data. Such a model was

also inconsistent with our analysis of 5-HT resensitization that suggested three or four kinetically equivalent rate-limiting steps. Allowing gating to occur with four agonist binding sites occupied increased the number of receptor states in our minimum model but did not improve its performance. We also found that, for some kinetic parameters, a range of values could reasonably reproduce our electrophysiological data. In particular, the values of the resting state agonist association and dissociation rate constants (k_1 and k_2) are order of magnitude estimates from the 5-HT concentration dependence of the rate of activation. However, the values of the other kinetic parameters could be estimated with greater precision. For example, the open and desensitized agonist dissociation rate constants (k_3) for 5-HT and DA could be narrowly defined by the time courses of resensitization (for 5-HT) and deactivation (for DA). Similarly, the desensitization rate constant (k_{d+}) was well

defined by the maximum rate of desensitization evoked by high 5-HT concentrations.

We note that, in some cases, our predictions deviated from experimental results. In particular, the recovery from DA-induced desensitization occurs with a time course that is more complex than that predicted by our model. This could reflect the existence of additional desensitized states not considered by our model that recover at different rates. The presence of additional states may also explain why the EC₅₀ values for desensitization predicted by our model are twofold lower than that determined from experimental data.

Our electrophysiological results and kinetic model for describing 5-HT_{3A} receptor function may be compared with those reported by other groups. Based on the results of electrophysiological studies of 5-HT action on murine 5-HT_{3A} receptors, Mott et al. (2001) proposed a kinetic model that differs from ours in several critical aspects. First, open and desensitized states do not exist in the absence of agonist in their model. Second, activation can occur when more than three agonist molecules are bound. Third, desensitization occurs only from the resting state. Fourth, the agonist affinity of the open state is infinitely high and the only route out of the open state is by returning to the preopen state. Fifth, the agonist affinities of resting and desensitized states are the same. In addition to proposing a different model, their approach to defining rate constants differed from ours. Rather than using many agonist concentrations and applying multiple experimental protocols to tease out the values of rate constants, Mott et al. estimated their values by simultaneously fitting averaged current traces evoked by the prolonged application of two concentrations of 5-HT directly to their scheme. Their model accurately simulated these two traces; however, traces impacted by the rates of deactivation, recovery from deactivation, or resensitization were not included in the fitting routine.

In another study of 5-HT action on 5-HT_{3A} receptors, Hapfelmeier et al. (2003) observed “tail currents” on the rapid termination of 5-HT indicative of open-channel block and proposed a relatively simple linear-branched kinetic scheme of receptor function. In their model, channel blockade drives desensitization. Because we rarely observed tail currents on withdrawal

of 5-HT and only at the highest agonist concentrations, we did not incorporate this feature into our scheme.

In summary, our studies of human 5-HT_{3A} receptors show that 5-HT and DA differ in their EC₅₀ values for peak current activation, efficacies, rates of current activation, EC₅₀ values for desensitization, maximum rates of desensitization, rates of resensitization, and rates of deactivation. Within the context of an allosteric kinetic model of 5-HT_{3A} receptor function, these many differences can be primarily attributed to the vastly different rates with which these two agonists induce channel opening and dissociate from open and desensitized states.

References

- Barnes JM, Barnes NM, Champaneria S, Costall B, Naylor RJ (1990a) Characterisation and autoradiographic localisation of 5-HT₃ receptor recognition sites identified with [³H]-(-S)-zacopride in the forebrain of the rat. *Neuropharmacology* 29:1037–1045.
- Barnes JM, Barnes NM, Costall B, Deakin JF, Ironside JW, Kilpatrick GJ, Naylor RJ, Rudd JA, Simpson MD, Slater P, Tyers MB (1990b) Identification and distribution of 5-HT₃ recognition sites within the human brainstem. *Neurosci Lett* 111:80–86.
- Beato M, Groot-Kormelink PJ, Colquhoun D, Sivilotti LG (2004) The activation mechanism of alpha1 homomeric glycine receptors. *J Neurosci* 24:895–906.
- Chang Y, Weiss DS (1998) Substitutions of the highly conserved M2 leucine create spontaneously opening rho1 gamma-aminobutyric acid receptors. *Mol Pharmacol* 53:511–523.
- Chang Y, Weiss DS (1999a) Allosteric activation mechanism of the alpha1beta2gamma2 gamma-aminobutyric acid type A receptor revealed by mutation of the conserved M2 leucine. *Biophys J* 77:2542–2551.
- Chang Y, Weiss DS (1999b) Channel opening locks agonist onto the GABAC receptor. *Nat Neurosci* 2:219–225.
- Chang Y, Ghansah E, Chen Y, Ye J, Weiss DS (2002) Desensitization mechanism of GABA receptors revealed by single oocyte binding and receptor function. *J Neurosci* 22:7982–7990.
- Changeux J, Edelman SJ (2001) Allosteric mechanisms in normal and pathological nicotinic acetylcholine receptors. *Curr Opin Neurobiol* 11:369–377.
- Costall B, Naylor RJ (2004) 5-HT₃ receptors. *Curr Drug Targets CNS Neurol Disord* 3:27–37.
- Edelman SJ, Schaad O, Henry E, Bertrand D, Changeux JP (1996) A kinetic mechanism for nicotinic acetylcholine receptors based on multiple allosteric transitions. *Biol Cybern* 75:361–379.
- Farber L, Haus U, Spath M, Drechsler S (2004) Physiology and pathophysiology of the 5-HT₃ receptor. *Scand J Rheumatol Suppl* 2–8.
- Forman SA (1999) A hydrophobic photolabel inhibits nicotinic acetylcholine receptors via open-channel block following a slow step. *Biochemistry* 38:14559–14564.
- Grosman C, Auerbach A (2001) The dissociation of acetylcholine from open nicotinic receptor channels. *Proc Natl Acad Sci USA* 98:14102–14107.
- Hapfelmeier G, Tredt C, Haseneder R, Zieglgansberger W, Eisensamer B, Rupprecht R, Rammes G (2003) Co-expression of the 5-HT_{3B} serotonin receptor subunit alters the biophysics of the 5-HT₃ receptor. *Biophys J* 84:1720–1733.
- Haus U, Spath M, Farber L (2004) Spectrum of use and tolerability of 5-HT₃ receptor antagonists. *Scand J Rheumatol Suppl* 12–18.
- Hodge CW, Kelley SP, Bratt AM, Iller K, Schroeder JP, Besheer J (2004) 5-HT_{3A} receptor subunit is required for 5-HT₃ antagonist-induced reductions in alcohol drinking. *Neuropsychopharmacology* 29:1807–1813.
- Hu XQ, Lovinger DM (2005) Role of aspartate 298 in mouse 5-HT_{3A} receptor gating and modulation by extracellular Ca²⁺. *J Physiol (Lond)* 568:381–396.
- Hu XQ, Sun H, Peoples RW, Hong R, Zhang L (2006) An interaction involving an arginine residue in the cytoplasmic domain of the 5-HT_{3A} receptor contributes to receptor desensitization mechanism. *J Biol Chem* 281:21781–21788.
- Johnson BA (2004) Role of the serotonergic system in the neurobiology of alcoholism: implications for treatment. *CNS Drugs* 18:1105–1118.
- Koshland Jr DE, Nemethy G, Filmer D (1966) Comparison of experimental binding data and theoretical models in proteins containing subunits. *Biochemistry* 5:365–385.
- Lovinger DM, Sung KW, Zhou Q (2000) Ethanol and trichloroethanol alter gating of 5-HT₃ receptor-channels in NCB-20 neuroblastoma cells. *Neuropharmacology* 39:561–570.
- Maconochie DJ, Steinbach JH (1998) The channel opening rate of adult- and fetal-type mouse muscle nicotinic receptors activated by acetylcholine. *J Physiol (Lond)* 506:53–72.
- Maconochie DJ, Zempel JM, Steinbach JH (1994) How quickly can GABAA receptors open? *Neuron* 12:61–71.
- McBride WJ, Lovinger DM, Machu T, Thielen RJ, Rodd ZA, Murphy JM, Roache JD, Johnson BA (2004) Serotonin-3 receptors in the actions of alcohol, alcohol reinforcement, and alcoholism. *Alcohol Clin Exp Res* 28:257–267.
- Mochizuki S, Miyake A, Furuichi K (1999) Ion permeation properties of a cloned human 5-HT₃ receptor transiently expressed in HEK 293 cells. *Amino Acids* 17:243–255.
- Monod J, Wyman J, Changeux JP (1965) On the nature of allosteric transitions: a plausible model. *J Mol Biol* 12:88–118.
- Mott DD, Erreger K, Banke TG, Traynelis SF (2001) Open probability of homomeric murine 5-HT_{3A} serotonin receptors depends on subunit occupancy. *J Physiol (Lond)* 535:427–443.
- Ortells MO, Lunt GG (1995) Evolutionary history of the ligand-gated ion-channel superfamily of receptors. *Trends Neurosci* 18:121–127.
- Peters JA, Hales TG, Lambert JJ (2005) Molecular determinants of single-channel conductance and ion selectivity in the Cys-loop family: insights from the 5-HT₃ receptor. *Trends Pharmacol Sci* 26:587–594.
- Purohit Y, Grosman C (2006) Estimating binding affinities of the nicotinic receptor for low-efficacy ligands using mixtures of agonists and two-dimensional concentration-response relationships. *J Gen Physiol* 127:719–735.
- Reeves DC, Lumms SC (2002) The molecular basis of the structure and function of the 5-HT₃ receptor: a model ligand-gated ion channel (review). *Mol Membr Biol* 19:11–26.
- Reeves DC, Jansen M, Bali M, Lemster T, Akabas MH (2005) A role for the beta 1-beta 2 loop in the gating of 5-HT₃ receptors. *J Neurosci* 25:9358–9366.
- Robert A, Howe JR (2003) How AMPA receptor desensitization depends on receptor occupancy. *J Neurosci* 23:847–858.
- Rusch D, Forman SA (2005) Classic benzodiazepines modulate the open-close equilibrium in alpha1beta2gamma2L gamma-aminobutyric acid type A receptors. *Anesthesiology* 102:783–792.
- Rusch D, Zhong H, Forman SA (2004) Gating allostereism at a single class of etomidate sites on alpha1beta2gamma2L GABA A receptors accounts for both direct activation and agonist modulation. *J Biol Chem* 279:20982–20992.
- Scheller M, Forman SA (2002) Coupled and uncoupled gating and desensitization effects by pore domain mutations in GABA_A receptors. *J Neurosci* 22:8411–8421.
- Solt K, Stevens RJ, Davies PA, Raines DE (2005) General anesthetic-induced channel gating enhancement of 5-hydroxytryptamine type 3 receptors depends on receptor subunit composition. *J Pharmacol Exp Ther* 315:771–776.
- Steward LJ, West KE, Kilpatrick GJ, Barnes NM (1993) Labelling of 5-HT₃ receptor recognition sites in the rat brain using the agonist radioligand [³H]meta-chlorophenylbiguanide. *Eur J Pharmacol* 243:13–18.
- van Hooft JA, Vijverberg HP (1996) Selection of distinct conformational states of the 5-HT₃ receptor by full and partial agonists. *Br J Pharmacol* 117:839–846.
- Yang J, Cheng Q, Takahashi A, Goubaeva F (2006) Kinetic properties of GABA rho1 homomeric receptors expressed in HEK293 cells. *Biophys J* 91:2155–2162.